

# Broken rotor bar detection of three phase induction motor using frequency response analysis

Rizwanullah Khan<sup>1</sup>, Mohd Fairouz Mohd Yousof<sup>1</sup>, Rahisham Abd Rahman<sup>1</sup>, Norhafiz Azis<sup>2</sup>,  
Salem Al-Ameri<sup>3</sup>, Asjad Ali<sup>4</sup>

<sup>1</sup>Faculty of Electrical and Electronic Engineering, Universiti Tun Hussein Onn Malaysia, Batu Pahat, Malaysia

<sup>2</sup>Faculty of Engineering, Universiti Putra Malaysia, Serdang, Malaysia

<sup>3</sup>Department of Electrical Engineering, Cutin University Malaysia, Miri, Malaysia

<sup>4</sup>Department of Electrical Engineering, University of Engineering and Technology Taxila, Taxila, Pakistan

## Article Info

### Article history:

Received Jul 23, 2024

Revised Sep 28, 2024

Accepted Oct 23, 2024

### Keywords:

Broken rotor bar

Condition monitoring

Frequency response analysis

Induction motor

Non-invasive testing

Rotor fault detection

## ABSTRACT

Three phase induction motors (TPIMs) are broadly utilized for various applications in the industry, but they are prone to different faults that can affect their performance and reliability. One common fault is a broken rotor bar, which leads to vibration, noise, and reduced efficiency. Therefore, detecting and identifying this fault early is important to avoid further damage and reduce maintenance costs. This paper proposes a novel method using frequency response analysis (FRA) to diagnose broken rotor bars in a TPIM. The response of normal motor is measured to obtain the baseline. Subsequently, the rotor was inflected with physical damage to represent a broken rotor bar. By comparing normal and faulty rotors, the measurement shows that frequency response analysis is sensitive toward various fault severity based on the number of broken rotor bars.

*This is an open access article under the [CC BY-SA](https://creativecommons.org/licenses/by-sa/4.0/) license.*



## Corresponding Author:

Rizwanullah Khan

Faculty of Electrical and Electronic Engineering, Universiti Tun Hussein Onn Malaysia

86400 Batu Pahat, Malaysia

Email: rizwanullah4996@gmail.com

## 1. INTRODUCTION

Three phase induction motors (TPIMs) are extensively used in modern industrial applications. These motors account for approximately 85% of the energy consumed in the industrial sector [1]. However, due to their widespread use, these motors are prone to various faults. Sophisticated techniques are required to identify different faults [2]. An effective method for identifying and diagnosing faults is vital for the industry. It prevents unplanned shutdowns, reduces maintenance costs, and minimizes downtime. Failures in TPIMs often arise from faults in the motor's stator, rotor, or mechanical systems, such as bearings and shafts, or from external sources [3], [4]. Rotor related faults contribute to approximately 10% of induction motor failures [3], [5]. Numerous surveys have been carried out to assess the percentage of failures attributed to different motor components [6], [7]. It is observed that the rate of these faults varies with other factors like the size of the motor, type of application, and manufacturing. For instance, motors operating at medium voltages are more prone to broken bar and end ring faults compared to smaller motors [3]. When a fault occurs in one of the bars, the current shifts to the neighboring bars, leading to increased thermal and magnetic stresses on those bars [8]–[10]. Additionally, irregularities in the rotor circuit lead to an increase in the reverse magnetic field, which affects the harmonic content of the stator current and other motor parameters [11]. Consequently, the motor's performance and reliability are reduced [4].

Moreover, the broken bar faults produce vibrations in the shaft, possibly leading to bearing issues and rotor misalignment faults [11]. Hence, early detection and diagnosis of broken rotor bars (BRB) have become imperative for modern industries. A thorough review of recent literature on techniques for detecting and diagnosing BRB faults in both line-fed and inverter-fed motors is detailed in [12]. The review discusses the difficulties in diagnosis and identifies the indicators of BRB faults in the author used. Barrera *et al.* [13] proposed an active fault diagnosis method for detecting broken rotor bars by injecting a zero-sequence signal and analyzing diagnostic responses. Hwang *et al.* [14] presented a robust method for detecting broken rotor bars by monitoring rotor flux angles and using a fault detection algorithm based on a dynamic model. A two-step approach for BRB detection is proposed in [15] where the first step analyzes three-axis vibration signals using fractal dimension theory, and the second employs fuzzy logic for automatic fault diagnosis in transient and steady-state conditions. Morinigo-Sotelo *et al.* [16] proposes detecting BRB faults in TPIMs by analyzing music and zero-sequence currents, utilizing a high-resolution spectral method known as multiple signal classification. In the literature, only a few studies have explored the use of frequency response analysis (FRA) for diagnosing TPIMs. Uhrig *et al.* [17] investigated that turn-to-turn causes variation in the frequency response of TPIM. Perisse *et al.* [18] introduced a novel monitoring system capable of detecting minor variations in frequency resonances within the windings of an operational motor powered by an industrial inverter. In study [19], the frequency response of a TPIM was analyzed under both healthy and stator winding fault conditions. Brandt *et al.* [20] FRA was utilized to identify failures in electrical machines. A previous paper has proposed that a rotor inside the stator winding affects the FRA signatures [21]. Therefore, rotor faults can be diagnosed using FRA.

This paper presents a new method for diagnosing faults related to broken rotor bars in (TPIMs) by analyzing the FRA signature of both healthy and faulty rotor bars. The main focus of this paper is to demonstrate the versatility of the FRA technique, highlighting its capability to detect and identify broken rotor bars within the rotating machine. The study presents experimental results to support the proposed approach.

## 2. BROKEN ROTOR BAR

The rotor consists of a series of conductive bars, typically made of aluminum or copper, connected at each end-by-end ring, forming a squirrel-cage structure. These rotor bars create a rotating magnetic field that drives the motor. Rotor bar failure is common in induction motors. These faults can arise from various factors, such as excessive mechanical stress, overheating, or manufacturing defects. The failure of one or more rotor bars can lead to multiple operational problems. Symptoms might include unusual vibrations, increased noise, decreased efficiency, and, in severe cases, motor failure [22]. Despite not immediately causing motor failure, broken rotor bars can result in significant secondary problems [5]. When the rotor operates asymmetrically, it leads to imbalanced currents, fluctuations in torque, heightened losses, and a reduction in average torque [23]. Detecting and identifying broken rotor bars early is crucial to prevent further damage and costly downtime [24]. Once identified, repairing or replacing the affected rotor or motor is necessary to restore optimal performance and reliability. In some cases, preventive maintenance and regular inspections can help avoid such faults by identifying and addressing the underlying causes before the rotor bars break [25].

## 3. PROPOSED METHOD

This paper presents a new method for diagnosing faults related to broken rotor bars in TPIMs by analyzing the FRA of both healthy and faulty rotor bars. The method relies on the concept that a fault in any rotor bar disrupts the symmetry between two bars, resulting in a deviation in their FRA signatures as an indication of the fault. This philosophy underpins the proposed method. However, in practice, a significant challenge lies in separately measuring responses for healthy and damaged rotor components of a given motor for feasibility testing and method clarity. One possibility could be drilling the bar of the rotor and conducting the measurement of FRA. The proposed methodology is shown in the flowchart in Figure 1.

### 3.1. Healthy motor

Initially, the FRA test is conducted on the motor under optimal conditions with the rotor in a healthy state to establish a baseline. This involves measuring the FRA of the stator considering different phase connections, specifically  $U_1W_1$  and  $V_1W_1$ , to capture their unique FRA signatures. These baseline signatures serve as a reference for subsequent comparisons and analysis, enabling the identification of any deviations or anomalies that may arise due to developing faults within the rotor.

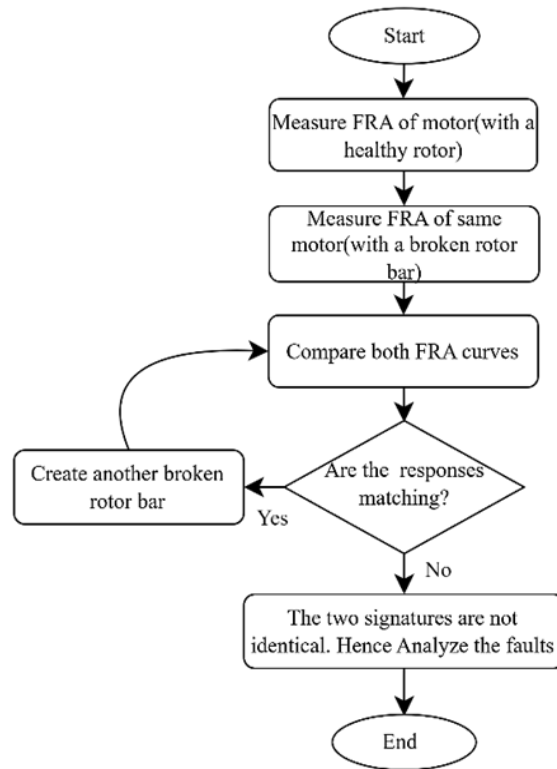


Figure 1. Flowchart of the methodology

### 3.2. Motor with broken bars

The motor's rotor bars were purposely damaged by drilling a 6-mm hole. The varying numbers of BRBs are illustrated in Figure 2. First, experiments were conducted with a rotor containing just one BRB, as shown in Figure 2(a). After recording the FRA signature, the rotor was removed and drilled again, resulting in two BRBs, as shown in Figure 2(b). Even though these were not real rotor failures, the artificially created broken bar has a specific FRA signature. This process was repeated till three BRBs, as shown in Figure 2(c). Furthermore, an artificial fault on the rotor was created by striking a rotor bar with a heavy hammer to create the common failure, which is rubbing in the rotor, as shown in Figure 2(d).

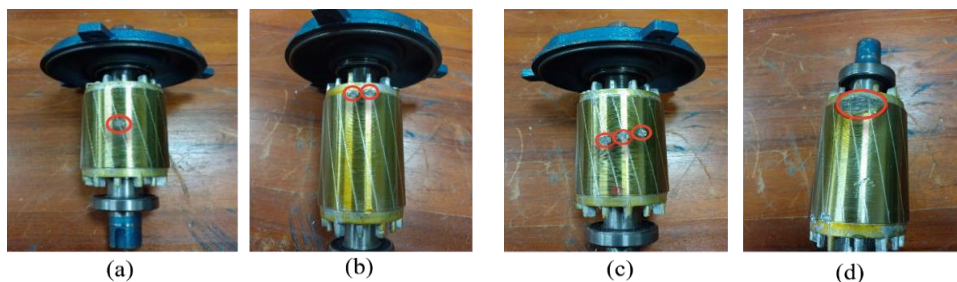


Figure 2. Rotor with (a) one broken bar, (b) two bars, (c) three bars, and (d) hit with a hammer

## 4. EXPERIMENTAL SETUP

A 3 HP TPIM is used. The motor has a total of 15 slots and a single-layer winding design. It has 16 rotor bars. The motor specifications used in the experimental work are shown in Table 1. First, the FRA signature is measured under normal rotor conditions using an FRA analyzer to obtain the baseline signature. Then, rotor bars are artificially broken using a hand drill. Two conditions of broken bars were created. In Condition 1, the bars were broken in the middle of the rotor, with up to three BRBs. In Condition 2, two consecutive bars were broken at the top ring of the rotor, followed by another pair at the bottom ring. The FRA response was observed for this configuration. Furthermore, an artificial fault on the rotor was created by

striking a rotor bar with a heavy hammer to simulate the common failure of rotor rubbing. The FRA response was also measured for this condition. After creating all possible artificial BRBs, their responses were compared with those of a healthy rotor and were analyzed. During the experimental work, two types of phase connections ( $U_1W_1$  and  $V_1W_1$ ) were considered. First, the measurement was taken between the  $U_1W_1$  terminals and the second between the  $V_1W_1$  terminals. The complete experimental setup (PC, three-phase induction motor, drill, and FRA measuring equipment) is shown in Figure 3.

Table 1. Specifications of motor

Specification	Value
No. Phases	3-Phase
Power	2.2 kW
Current	8.83 A
Efficiency	80.5%
Frequency	50 Hz
Voltage	380-420 V
Power factor	0.86
Pole pairs	2
Rated speed	2840 rpm

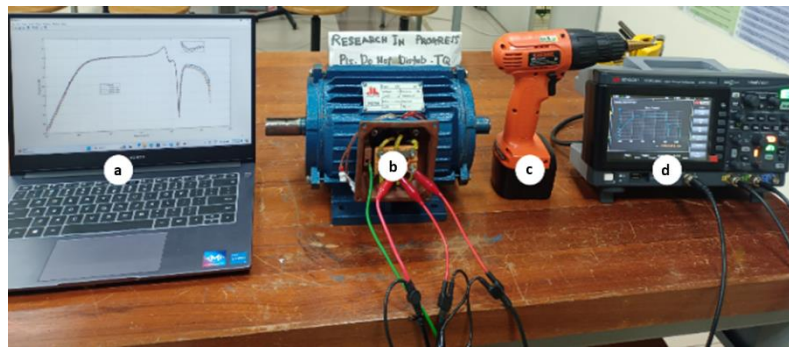


Figure 3. Experimental setup: (a) PC, (b) three phase induction motor, (c) drill, and (d) FRA measuring equipment

## 5. RESULTS AND DISCUSSION

This section presents and discusses FRA signatures for both motor with healthy rotor and BRBs within a frequency range of 10 Hz to 2 MHz. This range covers the dominant frequency regions affected by BRBs in the TPIM. The entire frequency range is segmented into smaller portions to analyze the impact of BRBs on FRA signatures precisely. Two types of results are presented: magnitude (dB) and phase ( $^{\circ}$ ) as shown in Figures 4 and 5. For the connection type  $U_1W_1$ , within the frequency range of 10 Hz to 10 kHz, a noticeable constant difference in FRA magnitude (dB) between healthy and BRBs is observed. As depicted in Figure 4(a), this difference increases as the number of BRBs increases. A similar change in magnitude and phase can be observed for different types of broken rotor bars (two consecutive bottom and top bars), as illustrated in Figure 4(b). Additionally, the number of BRBs affects the FRA signature phase ( $^{\circ}$ ), as shown in Figures 4(c) and 4(d).

As we move away from the 10 kHz frequency range, the FRA magnitude and phase difference between healthy and broken bars decrease. However, around 80 kHz, this difference begins to increase again. Between 80 and 120 kHz, the FRA curves for broken bars show a visible deviation from those of a healthy rotor, highlighted in the zoomed-in sections of Figure 4. In the frequency range of 120 to 170 kHz, a deviation is again observed between healthy and broken rotor bars. The maximum deviation is observed in the last frequency range, from 170 kHz to 2 MHz, representing the greatest deviation across the entire frequency range from 10 Hz to 2 MHz. The results in Figures 4(b) and 4(d) demonstrate that the FRA signature of a broken rotor due to rubbing exhibits similar effects to those of a rotor with an artificially drilled hole.

For the connection type ( $V_1W_1$ ), the same effect is observed across the frequency range as with the connection type ( $U_1W_1$ ). The comparison of results between a healthy rotor and a rotor with broken bars for connection type  $V_1W_1$  is illustrated in Figures 5(a) to 5(d). These figures show a clear FRA magnitude (dB) and phase difference between healthy and broken rotor bars in the 10 Hz to 10 kHz frequency range.

This variation becomes more noticeable with an increased number of broken bars. Above 10 kHz, the differences decrease but start increasing around 80 kHz and remain prominent up to 2 MHz. The results in Figures 5(b) and 5(d) indicate that the FRA signature of a broken rotor due to rubbing for connection type  $V_1W_1$  exhibits similar effects to those of a rotor with an artificially drilled hole.

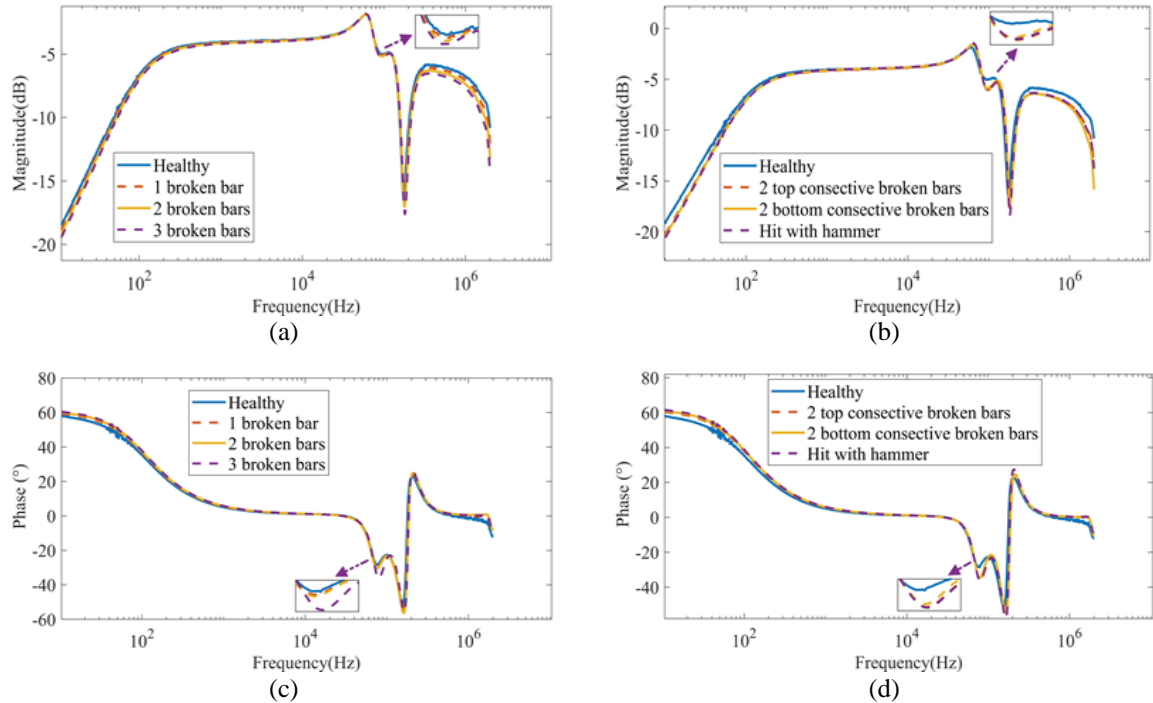


Figure 4. FRA results comparison for  $U_1W_1$  connection: (a) and (b) show magnitude (dB), (c) and (d) show phase (°)

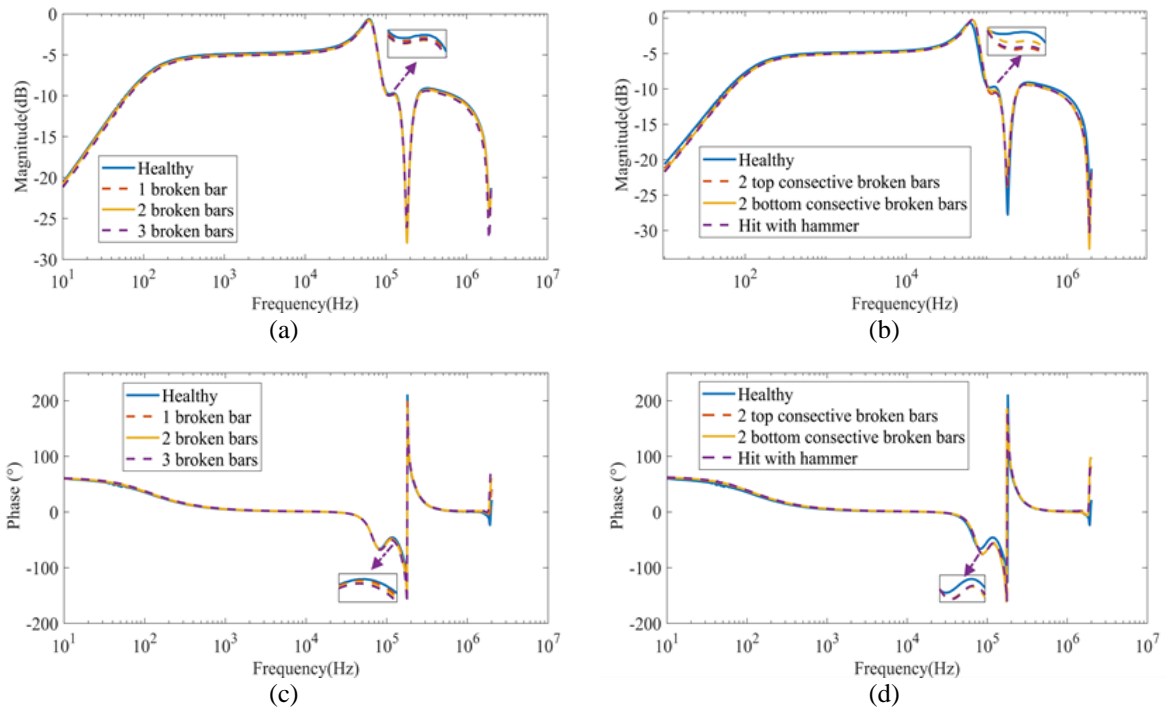


Figure 5. FRA results comparison for  $V_1W_1$  connection: (a) and (b) show magnitude (dB), (c) and (d) show phase (°)

A summary of the magnitude (dB) variation in FRA for healthy and broken rotors is provided in Tables 2 and 3. These numerical values are obtained from the results shown in Figures 4 and 5. Table 2 shows the magnitude (dB) variation for connection type  $U_1V_1$  for different broken bars. It can be seen from Table 2 that as the number of broken bars increases, the difference in magnitude (dB) also increases. Additionally, Table 2 shows that the variation in magnitude is not constant throughout the frequency range (10 Hz to 2 MHz). The difference in magnitude is more dominant in the frequency range of 120 to 170 kHz and minor in the range of 10 Hz to 10 kHz. A similar trend can be observed for connection type  $V_1W_1$ . Table 3 presents the numerical changes in magnitude for both healthy and varying numbers of broken bars. This data indicates that the number of broken bars significantly affects the FRA signature magnitude. The average difference for various numbers of broken bars in the frequency range of 10 to 80 kHz is shown in Table 3.

These findings suggest that broken rotor bars impact the motor's FRA regardless of the method used to induce such damage. This validates FRA as a reliable diagnostic tool for identifying rotor structural deficiencies, highlighting its sensitivity to blunt force impacts and precise modifications like drilling. Consequently, it provides invaluable insights to enhance the maintenance strategies for rotating machines.

Table 2. Magnitude (dB) comparison for  $U_1W_1$

Frequency	Healthy	1 BRB	2 BRB	3 BRB
10 Hz-10 kHz	-3.8	-3.85	-3.87	-3.89
10 kHz-80 kHz	-4.07	-4.12	-4.17	-4.22
80 kHz-120 kHz	5.04	-5.11	-5.18	-5.25
120 kHz-170 kHz	-16.35	-16.38	-16.41	-16.44
170 kHz-2 MHz	-6.06	-6.32	-6.58	-6.84

Table 3. Magnitude (dB) comparison for  $V_1W_1$

Frequency	Healthy	1 BRB	2 BRB	3 BRB
10 Hz-10 kHz	-2.32	-2.36	-2.44	-4.81
10 kHz-80 kHz	-4.52	-4.67	-4.67	-4.77
80 kHz-120 kHz	-9.8	-9.9	-9.99	-10
120 kHz-170 kHz	-22.06	-22.76	-22.86	-22.96
170 kHz-2 MHz	-9.62	-9.72	-9.8	-9.93

## 6. CONCLUSION

This paper investigates the effect of the broken rotor bar on the FRA signature of the TPIM. Experiments were conducted on a TPIM with different connection types, and the FRA patterns were analyzed for various broken bars. This paper presents an interesting finding that, although the rotor is not physically connected to the stator winding, the broken rotor bar influences the FRA signature, which is measured at the stator winding is significant. The results show that the rotor broken bar significantly impacts the FRA signature, particularly in the 120 to 170 kHz. Additionally, the results showed that the FRA pattern differs depending on the number of broken bars. This study establishes the FRA technique as a viable method for detecting faults within bars and assessing their severity. Furthermore, this research enhances the FRA technique's reputation as a reliable and non-intrusive diagnostic tool for maintaining induction motors, contributing to more effective and efficient preventive maintenance strategies.

## ACKNOWLEDGEMENTS

This research was supported by the Ministry of Higher Education (MOHE) through the Fundamental Research Grant Scheme FRGS/1/2022/TK07/UTHM/03/31.

## REFERENCES




- [1] E. Makhetha, M. Muteba, and D. V. Nicolae, "Effect of rotor bar shape and stator slot opening on the performance of three phase squirrel cage induction motors with broken rotor bars," in *Proceedings - 2019 Southern African Universities Power Engineering Conference/Robotics and Mechatronics/Pattern Recognition Association of South Africa, SAUPEC/RobMech/PRASA 2019*, 2019, pp. 463–468, doi: 10.1109/RoboMech.2019.8704850.
- [2] J. Rangel-Magdaleno, J. Ramirez-Cortes, and H. Peregrina-Barreto, "Broken bars detection on induction motor using MCSA and mathematical morphology: an experimental study," in *Conference Record - IEEE Instrumentation and Measurement Technology Conference*, 2013, pp. 825–829, doi: 10.1109/I2MTC.2013.6555530.
- [3] P. Zhang, Y. Du, T. G. Habetler, and B. Lu, "A survey of condition monitoring and protection methods for medium-voltage induction motors," *IEEE Transactions on Industry Applications*, vol. 47, no. 1, pp. 34–46, 2011, doi: 10.1109/TIA.2010.2090839.






- [4] H. Li, G. Feng, D. Zhen, F. Gu, and A. D. Ball, "A normalized frequency-domain energy operator for broken rotor bar fault diagnosis," *IEEE Transactions on Instrumentation and Measurement*, vol. 70, 2021, doi: 10.1109/TIM.2020.3009011.
- [5] W. T. Thomson and M. Fenger, "Current signature analysis to detect induction motor faults," *IEEE Industry Applications Magazine*, vol. 7, no. 4, pp. 26–34, 2001, doi: 10.1109/2943.930988.
- [6] S. B. Jiang, P. K. Wong, R. Guan, Y. Liang, and J. Li, "An efficient fault diagnostic method for three-phase induction motors based on incremental broad learning and non-negative matrix factorization," *IEEE Access*, vol. 7, pp. 17780–17790, 2019, doi: 10.1109/ACCESS.2019.2895909.
- [7] M. N. S. K. Shabbir, X. Liang, and S. Chakrabarti, "An ANOVA-based fault diagnosis approach for variable frequency drive-fed induction motors," *IEEE Transactions on Energy Conversion*, vol. 36, no. 1, pp. 500–512, 2021, doi: 10.1109/TEC.2020.3003838.
- [8] J. Faiz, V. Ghorbanian, and G. Joksimović, "Fault diagnosis of induction motors," *Fault Diagnosis of Induction Motors*, pp. 1–518, 2017, doi: 10.1049/pbpo108e.
- [9] G. Madescu, M. Biriescu, L. N. Tutelea, M. Mot, M. Svoboda, and I. Boldea, "Experimental investigation of rotor currents distribution in the healthy and faulty cage of induction motors at standstill," *IEEE Transactions on Industrial Electronics*, vol. 64, no. 7, pp. 5305–5313, 2017, doi: 10.1109/TIE.2017.2677337.
- [10] W. Li, Y. Xie, J. Shen, and Y. Luo, "Finite-element analysis of field distribution and characteristic performance of squirrel-cage induction motor with broken bars," *IEEE Transactions on Magnetics*, vol. 43, no. 4, pp. 1537–1540, 2007, doi: 10.1109/TMAG.2006.892086.
- [11] Z. Hosseinpoor, M. M. Arefi, R. Razavi-Far, N. Mozafari, and S. Hazbavi, "Virtual sensors for fault diagnosis: a case of induction motor broken rotor bar," *IEEE Sensors Journal*, vol. 21, no. 4, pp. 5044–5051, 2021, doi: 10.1109/JSEN.2020.3033754.
- [12] M. E. E. D. Atta, D. K. Ibrahim, and M. I. Gilany, "Broken bar fault detection and diagnosis techniques for induction motors and drives: State of the art," *IEEE Access*, vol. 10, pp. 88504–88526, 2022, doi: 10.1109/ACCESS.2022.3200058.
- [13] P. M. De La Barrera, M. Otero, T. Schallschmidt, G. R. Bossio, and R. Leidhold, "Active broken rotor bar diagnosis in induction motor drives," *IEEE Transactions on Industrial Electronics*, vol. 68, no. 8, pp. 7556–7566, 2021, doi: 10.1109/TIE.2020.3007108.
- [14] D. H. Hwang, Y. W. Youn, J. H. Sun, and Y. H. Kim, "Robust diagnosis algorithm for identifying broken rotor bar faults in induction motors," *Journal of Electrical Engineering and Technology*, vol. 9, no. 1, pp. 37–44, 2014, doi: 10.5370/jeet.2014.9.1.037.
- [15] J. P. Amezcua-Sanchez, M. Valtierra-Rodriguez, C. A. Perez-Ramirez, D. Camarena-Martinez, A. Garcia-Perez, and R. J. Romero-Troncoso, "Fractal dimension and fuzzy logic systems for broken rotor bar detection in induction motors at start-up and steady-state regimes," *Measurement Science and Technology*, vol. 28, no. 7, 2017, doi: 10.1088/1361-6501/aa6adf.
- [16] D. Morinigo-Sotelo, R. D. J. Romero-Troncoso, P. A. Panagiotou, J. A. Antonino-Daviu, and K. N. Gyftakis, "Reliable detection of rotor bars breakage in induction motors via MUSIC and ZSC methods," *IEEE Transactions on Industry Applications*, vol. 54, no. 2, pp. 1224–1234, 2018, doi: 10.1109/TIA.2017.2764846.
- [17] S. Uhrig, F. Öttl, N. Augeneder, and R. Hinterholzer, "Reliable diagnostics on rotating machines using FRA," *Lecture Notes in Electrical Engineering*, vol. 598 LNEE, pp. 738–751, 2020, doi: 10.1007/978-3-030-31676-1\_70.
- [18] F. Perisse, P. Werynski, and D. Roger, "A new method for AC machine turn insulation diagnostic based on high frequency resonances," *IEEE Transactions on Dielectrics and Electrical Insulation*, vol. 14, no. 5, pp. 1308–1314, 2007, doi: 10.1109/TDEL.2007.4339494.
- [19] T. G. Vilhekar, M. S. Ballal, and B. S. Umre, "Application of sweep frequency response analysis for the detection of winding faults in induction motor," *IECON Proceedings (Industrial Electronics Conference)*, pp. 1458–1463, 2016, doi: 10.1109/IECON.2016.7793565.
- [20] M. Brandt, M. Gutten, and S. Kaščák, "Diagnostic of induction motor using SFRA method," in *Proceedings of the International Conference - 2016 Conference on Diagnostics in Electrical Engineering, Diagnostika 2016*, 2016, pp. 1–4, doi: 10.1109/DIAGNOSTIKA.2016.7736474.
- [21] R. Khan, M. F. M. Yousof, R. Abd-Rahman, S. M. Al-Ameri, and N. Azis, "Impact of the rotor on FRA signatures and its implications for motor health assessment," in *2024 International Conference on Green Energy, Computing and Sustainable Technology, GECOST 2024*, 2024, pp. 364–369, doi: 10.1109/GECOST60902.2024.10474882.
- [22] O. E. Hassan, M. Amer, A. K. Abdelsalam, and B. W. Williams, "Induction motor broken rotor bar fault detection techniques based on fault signature analysis – A review," *IET Electric Power Applications*, vol. 12, no. 7, pp. 895–907, 2018, doi: 10.1049/iet-epa.2018.0054.
- [23] S. E. Zouzou, S. Khelif, N. Halem, and M. Sahraoui, "Analysis of induction motor with broken rotor bars using finite element method," *International Journal of Advance Engineering and Research Development*, vol. 3, no. 06, 2016, doi: 10.21090/ijaerd.030631.
- [24] G. A. Capolino, J. A. Antonino-Daviu, and M. Riera-Guasp, "Modern diagnostics techniques for electrical machines, power electronics, and drives," *IEEE Transactions on Industrial Electronics*, vol. 62, no. 3, pp. 1738–1745, 2015, doi: 10.1109/TIE.2015.2391186.
- [25] H. Henao *et al.*, "Trends in fault diagnosis for electrical machines: A review of diagnostic techniques," *IEEE Industrial Electronics Magazine*, vol. 8, no. 2, pp. 31–42, 2014, doi: 10.1109/MIE.2013.2287651.

## BIOGRAPHIES OF AUTHORS






**Rizwanullah Khan**    received a B.Eng. degree in electrical power engineering from UET, University of Engineering and Technology, Taxila, Pakistan, in 2022. He is currently pursuing an M.Eng. degree at UTHM, Universiti Tun Hussein Onn Malaysia. His research interests include fault diagnosis, condition monitoring, modeling, and design of electric machines and inverter drives. He can be contacted at email: rizwanullah4996@gmail.com.






**Mohd Fairouz Mohd Yousof**    obtained B.Eng. and M.Eng. degrees from Universiti Teknologi Malaysia and completed his Ph.D. from The University of Queensland, Australia. He is currently an associate professor at Universiti Tun Hussein Onn Malaysia. His main research is condition-based monitoring and assessment of high-voltage equipment, primarily power transformers and rotating machines. He is a member of IEEE and the Board of Engineers Malaysia. He can be contacted at email: fairouz@uthm.edu.my.






**Rahisham Abd Rahman**    received M.Eng. degree in electrical and electronic engineering from Cardiff University, UK in 2008. He received Ph.D. degree from Cardiff University, UK. He is currently an associate professor at Universiti Tun Hussein Onn Malaysia. His research interests include high voltage and energy systems. He can be contacted at email: rahisham@uthm.edu.my.






**Norhafiz Azis**    received the B.Eng. degree in electrical and electronic engineering from Universiti Putra Malaysia, Serdang, Malaysia, in 2007, and the Ph.D. degree in electrical power engineering from The University of Manchester, Manchester, United Kingdom. He is currently an associate professor with the department of electrical and electronic engineering at Universiti Putra Malaysia. His research interests are in-service transformer insulation aging, condition monitoring, asset management, and alternatives. He can be contacted at email: norhafiz@upm.edu.my.



**Salem Al-Ameri**    received B.Eng. in mechatronics engineering from Asia Pacific University (APU) in 2012. He received an M.Eng. in electrical from Universiti Tun Hussein Onn Malaysia (UTHM) in 2016. He received Ph.D. degree from The Universiti Tun Hussein Onn Malaysia in 2020. He is currently a lecturer at Curtin University, Malaysia. His research interests include transformer condition monitoring, high voltage, and renewable energy. He can be contacted at email: salem.mgammal@curtin.edu.my.



**Asjad Ali**    completed his bachelor's in electrical engineering from UET Taxila in 2022. His main interests include power systems, smart grids, power system planning and protection, and electrical machines. He has published articles related to smart grids and energy management. He can be contacted at email: asjadali14113@gmail.com.